Chapter 2

Relativistic stellar models of Compact objects

2.1 Introduction

Recent discovery of compact stellar objects leads to a concept that other than white dwarf, neutron stars there exists compact objects which may have configuration [6, 9, 10, 11, 15, 16, 17, 51, 52, 53] that need quarks as their constituents. The density of those compact objects is very high may be of the order of 10^{15} $g\ cm^{-3}$ or higher. The equation of State (EoS) of the compact objects are not precisely known yet. In GTR the Einstein field equation consists of two sectors, the gravitational and matter sectors. The conventional approach of obtaining models of relativistic stars in equilibrium heavily relies on the availability of definite information about the equation of state of its matter content. As a definitive equation of state inside a superdense strange star at present is not available we follow an alternative approach proposed by Vaidya-Tikekar [45] and Tikekar [46]. As discussed prescribing a suitable *ansatz* geometry for the interior physical 3-space of the configuration leads to simple easily tractable models of dense compact stars which are physically viable. Pant and Sah [50] obtained a class of relativistic static non-singular analytic solutions in isotropic form describing space time of static spherically symmetric distribution of matter in this approach. The solution has been found to lead to a physically viable causal model of neutron star with a maximum mass of $4M_{\odot}$.

In this chapter a class of general relativistic solutions for a class of compact stars which are in hydrostatic equilibrium are presented considering the isotropic form for a static spherically symmetric matter distribution. The general relativistic solutions obtained by Pant and Sah [50] are taken up here to examine physical plausibility of neutron stars with observed data of known stars. Since the field equation is highly non-linear we use numerical technique to explore the interior composition of compact star. In the model for known observed mass of compact object, the radius of the corresponding star is determined. In this model the variation of matter density on its boundary surface starting from the center of a superdense star for the prescribed geometry is studied.

2.2 Field Equation and Solution

We consider a static space time geometry in isotropic spherical polar coordinate, $(t,\ r,\ \theta,\ \phi)$, which is given by

$$ds^2 = e^{\nu(r)}dt^2 - e^{\mu(r)}(dr^2 + r^2 d\Omega^2) \tag{2.1}$$

with S^2 geometry is given by

$$d\Omega^2 = d\theta^2 + sin^2\theta \, d\phi^2, \tag{2.2}$$

where in eq.(1.6) we put $B^2(r) = e^{\mu}(r)$ and $A^2(r) = e^{\nu}(r)$. are metric potential at $t = constant$ hypersurface . The energy momentum tensor for a spherical distribution of matter in the form of perfect fluid in equilibrium is given by

$$T^{\mu}_{\mu} = diag\ (\rho, -p, -p, -p) \tag{2.3}$$

where ρ and p are energy density and fluid pressure of matter respectively. Using the space time metric given by eq.(2.2) , the Einstein's field eq.(1.1) in four-dimensions leads to the following equations :

$$\rho = -e^{-\mu}\left(\mu'' + \frac{\mu'^2}{4} + \frac{2\mu'}{r}\right) \tag{2.4}$$

$$p = e^{-\mu}\left(\frac{\mu'^2}{4} + \frac{\mu'}{r} + \frac{\mu'\nu'}{2} + \frac{\nu'}{r}\right) \tag{2.5}$$

$$p = e^{-\mu}\left(\frac{\mu''}{2} + \frac{\nu''}{2} + \frac{\nu'^2}{4} + \frac{\mu'}{2r} + \frac{\nu'}{2r}\right). \tag{2.6}$$

The pressure isotropy condition obtained from eq.(2.5) and eq.(2.6) leads to the following relation between metric variables μ and ν:

$$\nu'' + \mu'' + \frac{\nu'^2}{2} - \frac{\mu'^2}{2} - \mu'\nu' - \frac{1}{r}(\nu' + \mu') = 0. \tag{2.7}$$

The above eq.(2.7) is a second order differential equation in μ and ν, Pant and Sah obtained a simple solution [50] which is given by :

$$e^{\frac{\nu}{2}} = A_o\left(\frac{1 - k\alpha}{1 + k\alpha}\right), \qquad e^{\frac{\mu}{2}} = \frac{(1 + k\alpha)^2}{1 + \frac{r^2}{R^2}} \tag{2.8}$$

with

$$\alpha(r) = \sqrt{\frac{1+\frac{r^2}{R^2}}{1+\Lambda\frac{r^2}{R^2}}}. \tag{2.9}$$

where R, Λ, k and A_o are arbitrary constants. The above solution allows a geometry with 3-space that can be represented by a metric

$$d\sigma^2 = \frac{dr^2 + r^2(d\theta^2 + sin^2\theta d\phi^2)}{1+\frac{r^2}{R^2}} \tag{2.10}$$

It is a 3- sphere immersed in a 4-dimensional Euclidean space. Now, the geometry of physical space can be expressed as,

$$ds^2 = A_o^2\left(\frac{1-k\alpha}{1+k\alpha}\right)^2 dt^2 - \frac{(1+k\alpha)^4}{1+\frac{r^2}{R^2}}\left(dr^2 + r^2(d\theta^2 + sin^2\theta d\phi^2)\right). \tag{2.11}$$

It comes out that the geometry of the 3- space at $t = constant$ section of the space time metric eq.(2.11) shows a deviation introduced in spherical 3-space and k is a geometrical parameter measuring inhomogenity of the physical space. For $k = 0$, the space time metric eq.(2.11) , degenerates into that of Einstein's static universe which is filled with matter of uniform density. It is also evident that the condition $\Lambda = 0$, recovers the solution obtained by Buchdahl which is an analog of a classical polytrope of index 5. It is evident that the solution for $\Lambda > 0$, corresponds to finite boundary stellar models. Pant and Sah [50] obtained a class of non-singular analytic solution of the general relativistic field equations for a static spherically symmetric matter distribution. The solution is matched with Schwarzschild's empty space-time to study the behaviour of density and matter inside the star. In this chapter, stellar models for compact stars are presented to describe their physical properties taking into account the different values of the parameters R, Λ, k and A_o as permitted by the field equations.

The energy density and the pressure inside the star are obtained using eqs.(2.4)-(2.6) and eq.(2.11), which are given by

$$\rho = \frac{12(1+\Lambda k\alpha^5)}{R^2(1+k\alpha)^5}, \tag{2.12}$$

$$p = \frac{4(\Lambda k^2\alpha^6 - 1)}{R^2(1+k\alpha)^5(1-k\alpha)}. \tag{2.13}$$

The exterior Schwarzschild line element is

$$ds^2 = \left(1 - \frac{2M}{r_o}\right)dt^2 - \left(1 - \frac{2M}{r_o}\right)^{-1} dr^2 - r_o^2(d\theta^2 + sin^2\theta d\phi^2) \tag{2.14}$$

where m represents the mass of spherical object. To match the interior solution with the exterior solutions at the boundary we use the metric given by eq.(2.14) in an isotropic form [56]

$$ds^2 = \left(\frac{1 - \frac{M}{2r}}{1 + \frac{M}{2r}}\right)^2 dt^2 - \left(1 + \frac{M}{2r}\right)^4 (dr^2 + r^2 d\Omega^2) \tag{2.15}$$

by using the transformation $r_o = r\left(1 + \frac{M}{2r}\right)^2$ where r_o is the radius of the compact object.

2.3 Physical properties of a compact star

In this section we investigate physical features of compact objects using relativistic solution given by eq.(2.8) in a general way. The outline of the analysis is as follows:

(1) The energy density (ρ) and pressure (p) are determined from eq.(2.12) and eq.(2.13). It is noted that ρ is always positive for positive Λ and k, while positivity of pressure ($p \geq 0$) is permitted in the following cases:

Case(i): $\Lambda > \frac{1}{k^2\alpha^6}$ with $k < \frac{1}{\alpha}$

Case(ii): $\Lambda < \frac{1}{k^2\alpha^6}$ with $k > \frac{1}{\alpha}$.

(2) The interior solution is matched with the isotropic form of Schwarzschild exterior solution at the boundary of the star ($r = b$) which gives,

$$e^{\frac{\nu}{2}}|_{r=b} = \left(\frac{1-\frac{M}{2b}}{1+\frac{M}{2b}}\right) \qquad e^{\frac{\mu}{2}}|_{r=b} = \left(1+\frac{M}{2b}\right)^2 \tag{2.16}$$

(3) The physical radius of a star (r_o), is determined making use of the radial distance where the pressure at the boundary vanishes (i.e., $p(r) = 0$ at $r = b$). The physical radius is given by $r_o = b\left(1+\frac{M}{2b}\right)^2$ [56].

(4) The compactification factor ($\frac{M}{b}$) is determined using eqs.(2.8) and (2.15) which is given by

$$\frac{M}{b} = 2\left(\frac{1+k\alpha}{\sqrt{1+y^2}} - 1\right) \tag{2.17}$$

(5) The energy-density inside the star is always positive *i.e.*, ($\rho > 0$).

(6) The causality condition, $\frac{dp}{d\rho} < 1$ should be satisfied from the center to the boundary in order that the sound propagation to be causal.

To construct a stellar model we also consider that the usual boundary conditions *i.e.*, the first and second fundamental forms be continuous across the boundary ($r = b$). Making use of the boundary conditions as mentioned above one determines the unknown parameter A_o which is

$$A_o = \frac{\left(1-\frac{M}{2b}\right)}{\left(1+\frac{M}{2b}\right)}\left(\frac{\sqrt{1+\Lambda\frac{b^2}{R^2}} + k\sqrt{1+\frac{b^2}{R^2}}}{\sqrt{1+\Lambda\frac{b^2}{R^2}} - k\sqrt{1+\frac{b^2}{R^2}}}\right) \tag{2.18}$$

Now at the boundary ($r = b$), an eighth order polynomial equation in y ($y = \frac{b}{R}$) is emerged equating eqs.(2.8) and (2.15) at the boundary:

$$[(1+A_o)^4+k^4(1-A_o)^4-8(1+A_o)^2+16-2k^2(1-A_o^2)^2-8k^2(1-A_o)^2]+[2\Lambda(1+A_o)^4-16\Lambda(1+A_o)^2$$

$$-8(1+A_o)^2+32(1+\Lambda)-2k^2(1-A_o^2)^2(1+\Lambda)-8k^2(2+\Lambda)(1-A_o)^2+2k^4(1-A_o)^4]y^2$$

$$+[\Lambda^2(1+A_o)^4-8\Lambda^2(1+A_o)^2-8\Lambda(1+A_o)^2+(1+4\Lambda+\Lambda^2)-2\Lambda k^2(1-A_o^2)^2$$

$$-8k^2(1-A_o)^2(1+2\Lambda)+k^4(1-A_o)^4]y^4-[8\Lambda^2(1+A_o)^2-32(1+\Lambda)-8\Lambda k^2(1-A_o)^2]y^6+16\Lambda^2y^8=0 \tag{2.19}$$

where Λ, k and A_o are constants. Again by imposing the condition that pressure at the boundary vanishes in eq.(2.13), one can determine y as

$$y=\sqrt{\frac{1-(\Lambda k^2)^{1/3}}{(\Lambda k^2)^{1/3}-\Lambda}}. \tag{2.20}$$

It is noted that the size of a star is determined by k and Λ. It is also noted that a real y is permitted when (i) $k>\Lambda$ with $\Lambda<1$, or (ii) $k<\Lambda$ with $\Lambda>1$. Using eqs.(2.19) and (2.20), a polynomial equation in Λ, k and A_o is obtained. Although the eq.(2.19) is a polynomial of degree eight we found that only one realistic solution for y is obtained for different domains of the values of a pair of parameters namely, A_o, k and Λ. Subsequently the other parameters are also determined. For example, (i) when $A_o=2$, we found that Λ and k satisfy the following inequalities $2.9\le k\le 5$ and $1.4877\times10^{-6}\le\Lambda\le 0.04$, (ii) when $A_o=4$, the range of permitted values are $1.7\le k\le 2.3$ and $0.0185\le\Lambda\le 0.0653$. However, for a given Λ, e.g., (i) when $\Lambda=0.15$, the permitted values of A_o lies in the range $3.6<A_o<5.6$, and (ii) when $\Lambda=0.1318$, one obtains realistic solution for $3.5<A_o<5.8$.

The square of the acoustic velocity $\frac{dp}{d\rho}$ takes the form :

$$\frac{dp}{d\rho}=\frac{6\Lambda k\alpha^5(1-k\alpha)(1+k\alpha)-5(1-k\alpha)(\Lambda k^2\alpha^6-1)+(\Lambda k^2\alpha^6-1)(1+k\alpha)}{15(1-k\alpha)^2(\Lambda\alpha^4(1+k\alpha)-(1+\Lambda k\alpha^5))}. \tag{2.21}$$

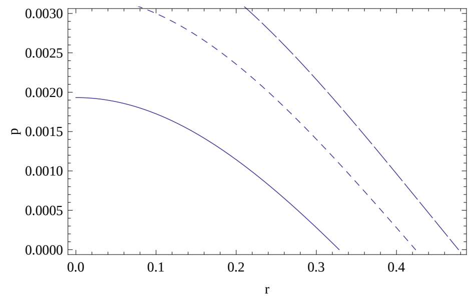

Figure 2.1: Variations of pressure with radial distance (in the unit of R) is plotted with solid line for $\Lambda = 0.15$, dashed line for $\Lambda = 0.1318$ and broken line for $\Lambda = 0.1211$.

The radial variation of $\frac{dp}{d\rho}$ for $\Lambda = 0.1318$ and $k = 2.2268$ is tabulated in Table- 2.1. It is evident that $\frac{dp}{d\rho}$ is maximum at the center and gradually decreases outward. It is also found that inside the star the constraint $\frac{dp}{d\rho} < 1$ is always satisfied which ensures causality. In Table- 2.2, variation of $\frac{dp}{d\rho}$ from the center to the boundary for different values of Λ and k are presented. It is evident that as Λ increases $\frac{dp}{d\rho}$ decreases at the center. The variation of the central density with Λ and k are displayed in Tables-2.3 and 2.4 for $A_o = 2$ and 4 respectively. It is found that the central density (ρ_c) decreases with an increase in Λ. It is also found that the stellar models with larger Λ accommodate a denser compact object compared to that for the lower values of Λ and k. The radial variations of pressure and density are drawn using eqs.(2.12) and (2.13) which are shown in figs.(2.1)-(2.4). Since it is not possible to express pressure in terms of density we study the behavior of pressure and density inside the curve numerically. In fig.(2.5) the variation of pressure with density is plotted for different model parameters.

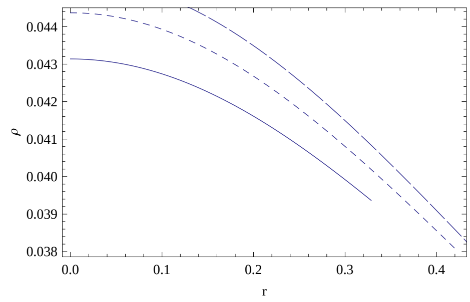

Figure 2.2: Variations of density with radial distance (in the unit of R) is plotted with solid line for $\Lambda = 0.15$, dashed line for $\Lambda = 0.1318$ and broken line for $\Lambda = 0.1211$.

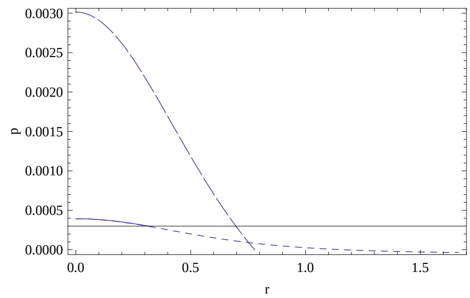

Figure 2.3: Variations of pressure with radial distance (in the unit of R) is plotted with solid line for $A_o = 4$, broken line for $A_o = 3$ and dashed line for $A_o = 2$.

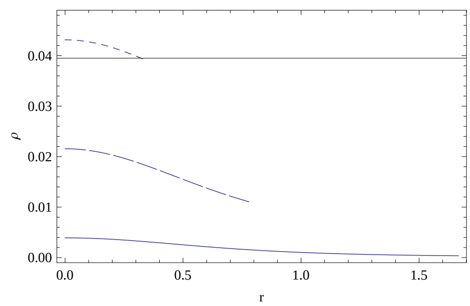

Figure 2.4: Variations of density with radial distance (in the unit of R km) is plotted with solid line for $A_o = 4$, broken line for $A_o = 3$ and dashed line for $A_o = 2$.

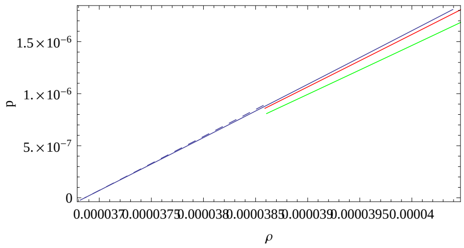

Figure 2.5: Variations of pressure with density is plotted with green line for $\Lambda = 0.0876$, red line for $\Lambda = 0.1318$, solid line for $\Lambda = 0.15$ and dashed line for $\Lambda = 0.165633$.

r in the unit of R	$\frac{dp}{d\rho}$
0	0.521
0.1	0.518
0.2	0.513
0.3	0.504
0.4	0.496
0.41	0.495
0.42	0.495

Table 2.1: Variation of $\frac{dp}{d\rho}$ with radial distance r for a given $\Lambda = 0.1318$ and $k = 2.2268$

r in the unit of R	$\frac{dp}{d\rho}$ for $\Lambda = 0.1211$ $k = 2.2$	$\frac{dp}{d\rho}$ for $\Lambda = 0.1318$ $k = 2.2268$	$\frac{dp}{d\rho}$ for $\Lambda = 0.15$ $k = 2.2681$
0	0.524	0.521	0.520
0.1	0.521	0.518	0.520
0.2	0.514	0.513	0.513
0.3	0.504	0.504	0.508
0.4	0.494	0.496	

Table 2.2: Variation of $\frac{dp}{d\rho}$ with radial distance r for different values of Λ and k.

2.4 Physical Analysis :

The physical properties of compact objects are numerically analyzed here. For a given values of Λ and k, the radial distance at which the pressure vanishes can

Λ	k	ρ_c in the unit of $\frac{1.9\times10^{15}}{R^2}$ kg/m^3
1.4877×10^{-6}	2.9	0.0133
1.3836×10^{-5}	3	0.0117
0.0048	4	0.0039
0.0400	5	0.0019

Table 2.3: Variation of central density for $A_o = 2$ for different values of Λ and k.

Λ	k	ρ_c in the unit of $\frac{1.9\times10^{15}}{R^2}$ kg/m^3
0.0185	1.7	0.0863
0.0289	1.8	0.0734
0.0432	1.9	0.0633
0.0876	2.1	0.0496
0.1211	2.2	0.0453
0.15	2.268	0.0431

Table 2.4: Variation of central density for $A_o = 4$ for different values of Λ and k

$A_o = 2$	M (mass) in $M_\odot$	r_o (radius) in km
$\Lambda = 1.48\times10^{-6}$, $k = 2.9$	3.61	12.087
$\Lambda = 1.17\times10^{-5}$, $k = 2.99$	2.69	9.250
$\Lambda = 1.38\times10^{-5}$, $k = 3.0$	2.63	9.067
$\Lambda = 3.93\times10^{-2}$, $k = 4.99$	0.12	0.622

Table 2.5: Variation of mass and radius of a compact star for different values of Λ and k for $R = 0.2$ km.

be determined from eq.(2.14). The mass to radius $\frac{M}{b}$ is estimated from eq.(2.18), which in turn determines the physical size of the compact star (r_o). For a given set of values of the parameters Λ, A_o and k, the mass (M) and radius of a compact object is obtained in terms of the model parameter R. For a given mass of a compact star, R is determined which further determines the corresponding radius. The field equations to determine the parameters are highly non-linear and intractable to a known functional

$A_o = 4$	M (mass) in $M_\odot$	r_o (radius) in km
$\Lambda = 0.1211$, $k = 2.2$	3.35	11.268
$\Lambda = 0.1318$, $k = 2.2268$	2.82	10.324
$\Lambda = 0.15$, $k = 2.2681$	2.45	8.409
$\Lambda = 8.76 \times 10^{-2}$, $k = 2.1$	4.19	13.688
$\Lambda = 0.1656$, $k = 2.3$	1.79	6.214

Table 2.6: Variation of mass and radius of a compact star for different values of Λ and k for $R = 2.5$ km.

Λ	1.48×10^{-6}	8.76×10^{-2}	0.1211	0.1318	0.15	0.1656
k	2.9	2.1	2.2	2.2268	2.2681	4.99
$\frac{\rho_b}{\rho_o}$	1.89×10^{-5}	0.45	0.54	0.58	0.69	0.81

Table 2.7: Variation of the ratio of the density at the boundary to the density at the center of a compact star for different values of Λ and k.

form. Hence, we adopt numerical technique in the next section.

In figs. (2.1)-(2.5) we plot the radial variation of pressure and density for different parameters. It is observed that as Λ is increased both the pressure and density of the compact object at the center decreases. It allows a massive star in a smaller radius for large Λ.

For a given mass of a compact star [15], known from observation, the parameter R is determined which further determines the radius. It is known that the radius of a neutron star is less than (11-14) km. [57], it is possible to obtain a class of stellar models for different values of R so that the size of a star never exceeds the upper bound. In the next section we discuss five different stellar models using stellar mass data [15, 41, 58].

Model 1 : An X-ray pulsar Her X-1 [15, 59] which is characterized by mass $M = 1.47\ M_\odot$, where $M_\odot$ = the solar mass, can be accommodated with a radius

$r_o = 4.921$ km., for $R = 0.081$ km. The compactness of the star in this case is $u = \frac{M}{r_o} = 0.30$. The ratio of density at the boundary to that at the center for the star is 0.0003 which is permitted for the parameter values, $\Lambda = 1.48 \times 10^{-6}$ and $k = 2.9$. Taking different values of R we get different models but a physically realistic model is obtained which accommodates a compact star with radius ~ 10 km. For example, if $R = 2.504$ km., one obtains a compact object with radius $r_o = 7.791$ km. In the latter case the ratio of density at the boundary to that at the center is found very high (0.99). The compactness of the star is 0.189 which is permitted for the parameters $\Lambda = 0.0393$ and $k = 4.99$ with $A_o = 2$.

Model 2 : An X-ray pulsar 4U 1700- 37 which is characterized by mass $M = 2.44\ M_\odot$ [15], can be accommodated with a radius $r_o = 8.197$ km. when $R = 1.819$ km., $A_o = 4$, $\Lambda = 0.1211$ and $k = 2.2$. The ratio of density at the boundary to that at the center for the star is 0.820. However, for the set of parameters with $A_o = 2$, $\Lambda = 0.1656$ and $k = 2.3$, a compact object can be accommodated with different radius $r_o = 8.110$ km. when $R = 0.135$ km. The ratio of density at the boundary to that at the center for the star in the later case is 0.0003. One obtains a star where the ratio of density at the boundary to that at the center is 0.99 when $A_o = 2$, $\Lambda = 0.0393$ and $k = 4.99$. In the later case the density profile value is found to be more compared to that of the former model with $A_o = 4$. However, in both the cases the compactness factor is $u = 0.3$.

Model 3 : A neutron star J1518+4904 of mass $M = 0.72\ M_\odot$ [15] can be accommodated with radius of $r_o = 2.419$ km. when $R = 0.537$ km. with $\Lambda = 0.1211$, $k = 2.2$ and $A_o = 4$. The ratio of density at the boundary to that at the center for the star is 0.82. The compactness factor of the star is $u = 0.3$. For $A_o = 2$ we note the following cases:

(i) when $\Lambda = 1.48 \times 10^{-6}$ and $k = 2.9$, it permits a star with radius $r_o = 2.4$ km. for $R = 0.04$ km. and (ii) when $\Lambda = 0.0393$ and $k = 4.99$, it permits a star with radius $r_o = 3.816$ km. for $R = 1.226$ km. The ratio of density at the boundary to that at the center for the star in the first case is 0.0003 and that in the later case is 0.988. However, the compactness factor for the former model is 0.3 which is higher than that for the later case (0.189).

Model 4 : A neutron star J1748-2021 B of mass $M = 2.74\ M_{\odot}$ [15] of radius $r_o = 9.281$ km. can be accommodated when $R = 2.247$ km. with $A_o = 4$, $\Lambda = 0.1318$ and $k = 2.2268$. The ratio of density at the boundary to that at the center for the star is 0.856 and the compactness factor in this case is $u = 0.3$. For $A_o = 2$, stellar model admits a star with radius $r_o = 13.154$ km. for $R = 2.74$ km, $\Lambda = 0.138 \times 10^{-5}$ and $k = 3$. However a star with smaller radius $r_o = 8.380$ km. can be accommodated here when $R = 0.181$ km. with $\Lambda = 1.17 \times 10^{-5}$ and $k = 2.99$. The ratio of density at the boundary to that at the center in the first case is 0.0017 which is found higher than the later (0.0015). The compactness factor in the former model is 0.20 which is smaller than the later one which is 0.32.

2.5 Discussions :

A relativistic solution for a class of compact stars which are in hydrostatic equilibrium is obtained considering isotropic form of a static spherically symmetric matter distribution. It may be pointed out here that Pant and Sah [50] obtained relativistic solution for neutron stars. Using Pant and Sah solution we study stellar models for varieties of compact objects discovered in recent times. The use of observed stellar data in relativistic stellar model is reported in [15]. Considering the isotropic form of the exterior Schwarzschild solution, Pant and Sah solution is matched at the boundary of the compact object to explore stellar models. The stellar models contains four unknown parameters Λ, A_o, k and R. The observed mass of a star determines R for given values of Λ, A_o, k. We note the following: (i) In fig. (2.1), variation of pressure with radial distance is plotted for different Λ for given values of A_o and k. The figures show that as Λ increases pressure inside the star decreases from the center to the boundary. (ii) In fig. (2.2), radial variation of density is plotted for different Λ. A higher density for lower Λ is noted in this case. (iii) The variation of $\frac{dp}{d\rho}$ inside the star for a given set of values of Λ and k are shown in Table-2.1. The causality condition is obeyed inside the star and the square speed of sound ($\frac{dp}{d\rho}$) attains a maximum at the center which however found to decrease monotonically radially outward. For different Λ and k, values of $\frac{dp}{d\rho}$ is shown in Table- 2.2. It is evident that $\frac{dp}{d\rho}$ decreases for an increase in Λ and k values. (iv) Variation of central density for different values of Λ and k with $A_o = 2$ and $A_o = 4$ are presented separately in Tables- (2.3) and (2.4) respectively. We note that the central density decreases as the value for the pair (Λ and k) increases. From Tables- (2.3) and (2.4) similar tendency for central density is found to exist when A_o is increased. As the isotropic Schwarzschild metric is singular at $M = 2b$, the model considered here may be useful to describe a strange star with $M \neq 2b$ or $M < 2b$. (v) In Tables- (2.5) and (2.6), the mass of a star with its maximum size is shown for different values of Λ and k taking density of a star

$\rho_b = 2 \times 10^{15}\ gm/cc$ at the boundary. We obtain here a class of relativistic stellar models for different values of Λ, A_o, k and R. (vi) The density profile of a given star with different values of Λ and k is shown in Table- 2.7. As Λ increases the ratio of density at the boundary to that at the center is found to increase accommodating more compact stars. (vii) In fig. (2.3), the variation of pressure with radial distance is plotted for different values of A_o. It is evident that as A_o increases pressure decreases. (viii) In fig. (2.4), variation of density with radial distance is plotted for different A_o. We note that as A_o is increased both the density and the pressure decreases. But the size of a star increases with an increase in A_o thereby accommodating more compact stars. (ix) In fig. (2.5), variation of pressure with density is plotted for different Λ. We note that for a given density, pressure is more for higher Λ, accommodating a star with higher central density.

Models of neutron stars that are investigated for some known compact objects for the relativistic solutions are discussed in section 4. As the equation of state is not known we analyze the star for known geometry, here Pant and Sah [50] metric is considered. The radii of the compact stars namely, neutron stars are also estimated here for known mass with a given R. The parameter R permits a class of compact objects, some of which are relevant observationally. Considering observed masses of the compact objects namely, X-ray pulsars Her X-1, 4U 1700-37 and neutron stars J1518+4904, J1748-2021 B we analyze the interior of the star. We obtain a class of compact stars models for various R with given values of k, Λ and A_o. The stellar models obtained here is found to accommodate highly compact objects.